Contents list available at IJRED website

Int. Journal of Renewable Energy Development (IJRED)

Journal homepage: http://ejournal.undip.ac.id/index.php/ijred

Research Article

Advanced Loop Thermosiphon With Check Valve (ALT/CV): Thermal Performance and Behavior

Khridsadakhon Booddachan, Nipon Bhuwakietkumjohn, Thanya Parametthanuwat*

Heat Pipe and Nanofluid Technology Research Unit, King Mongkut's University of Technology North Bangkok, Thailand

ABSTRACT. Nanofluids (NFs) are an attractive alternative to traditional working fluids for thermosiphons, but the solid nanoparticles (NPs) within the NF can agglomerate and reduce the thermal performance. This study focused on clarifying the effect of a NF with surfactants on the heat transfer characteristics of an advanced loop thermosiphon with a check valve (ALT/CV). In an experiment, the ALT/CV was filled with different working fluids at filling ratios of 30%, 50%, and 80% with respect to the evaporator volume. Heat was supplied at 20%, 40%, 60%, 80%, and 100% of the heater output (2000 W). Five working fluids were considered: deionized (DI) water, a DI water-based NF with 0.5 wt% silver NPs, and the same NF containing 0.5, 1, and 1.5 wt% oleic acid (OA) and potassium oleate (OAK^+) as surfactants. The results showed that the ALT/CV provided a better heat transfer performance than a normal thermosiphon. The maximum heat transfer rate was achieved with the NF containing 0.5 wt% silver NPs and 1 wt% OAK^+. The NF containing OAK^+ demonstrated a heat transfer rate approximately 80% higher than that of the DI water.

Keywords: Loop thermosiphon, Check valve, Nanofluids, Surfactant, Potassium oleate

Article History: Received: 28th October 2020; Revised: 17th December 2020; Accepted: 31st Dec 2020; Available online: 2nd Jan 2021
How to Cite this Article: Bhuwakietkumjohn, N., Booddachan, K., and Parametthanuwat, T., (2021) Advanced loop thermosiphon with check valve (ALT/CV): Thermal performance and behavior. *Int. Journal of Renewable Energy Development*, 10(2), 283-295
https://doi.org/10.14710/ijred.2021.33805

1. Introduction

Previous studies have used the two-phase closed thermosiphon (TPCT) as a heat exchanger (Payakaruk *et al.,* 2000; Ristoiu *et al.,* 2003; Sözen *et al.,* 2019) for applications such as solar power systems, cooling systems, engine cooling, electronic conductors, and heat waste recycling. As shown in Figure 1(A), a TPCT consists of three sections: an evaporator, adiabatic, and condenser section. The evaporator receives heat from the heat source and evaporates the working fluid inside the adiabatic section. The adiabatic section is not involved in the heat transfer and may be omitted from analysis. In the condenser, the vaporized working fluid releases heat to the heat receptor and condenses into a liquid (Bhuwakietkumjohn *et al.,* 2015; Lock, 1992; Noie *et al.,* 2007). The TPCT has two major problems. First, when pool boiling occurs, the vapor floats to the condenser section and condenses, which causes the liquid to flow back to the inner edge of the TPCT walls and then fall down because of gravity. This causes the liquid and vapor to collide, which reduces the heat transfer performance (Bhuwakietkumjohn *et al.,* 2017). This also thickens the liquid film on the TPCT wall, which increases the total thermal resistance (Z_{total}) and reduces the heat transfer rate (Lock, 1992; Reay *et al.,* 2006; Terdtoon *et al.,* 1998). Second, traditional working fluids such as water and ethanol are unsuitable for use in a TPCT because of their poor physical properties, which cause difficulties during the phase change (Choi, 1995; Yu *et al.,* 2007).

The first problem can be solved by reducing the collision between the liquid and vapor. Figure 1(B) shows the design of an advanced loop thermosiphon with a check valve (ALT/CV), which transforms the traditional TPCT into a loop TPCT (Jengsooksawat *et al.,* 2008; Vincent et al., 1992). This design still features the original physical characteristics of the TPCT but adds a check valve to control the direction of the vapor flow (Rittidech *et al.,* 2007) and improve the heat transfer performance. The second problem can be solved by adding nanoparticles (NPs) to a traditional working fluid to produce a nanofluid (NF) (Choi 1995; Kang *et al.,* 2009; Khandekar *et al.,* 2008). Adding NPs improves the thermodynamic physical properties of traditional working fluids, including the density, specific heat capacity, and thermal conductivity (Buongiorno *et al.,* 2009); this also improves the heat transfer performance (Choi 1995; Sharma *et al.,* 2011). However, the solid-state particles in an NF may precipitate, coagulate, or form clusters, which can significantly reduce the heat transfer performance (Hwang *et al.,* 2008). Therefore, a suitable NF preparation technique needs to be devised. Researchers use different methods depending on the base fluid, NF, and NPs. Different reports in the literature have shown that adding NPs does not increase the heat capacity of an NF (Starace *et al.,* 2011). The most important factors appear to be the effective particle concentration, shear rate, viscosity of the

* Corresponding author: Thanya.P@fitm.kmutnb.ac.th

base liquid, physical properties, preparation method, and controlled conditions (Buongiorno *et al.,* 2009). Thus, the vast differences among different experimental conditions need to be considered when determining a suitable preparation method and NP concentration.

Silver NPs are traditionally used in NFs because silver has the highest thermal conductivity in the transition metal group (Buongiorno *et al.,* 2009; Michaelides *et al.,* 2016; Parametthanuwat *et al.,* 2013). Compared to most solids, silver NPs have the potential to be a good stabilizer and can improve the thermal performance of the base fluid. However, reducing the lead time for uniform dispersion of NPs may cause them to form agglomerations in the NF (Hwang *et al.,* 2008; Mahbubul, 2019).

Surfactants have been used to reduce the surface tension of traditional working fluids and support smaller particles for greater distribution. To reduce coagulation, the two-step method is used to increase the wave frequency, accelerate the particle dispersion, and control the temperature below 20°C (Hwang *et al.,* 2008). This improves the rheological behavior of the working fluid (Chen *et al.,* 2007; Parametthanuwat *et al.,* 2015). Oleic acid (OA) and potassium oleate (OAK^+) reduce the surface tension and increase the homogeneity of the dispersed NPs (Radiom *et al.,* 2013; Warrier *et al.,* 2011). Thus, silver NPs with OA and OAK^+ can increase the thermal conductivity and heat transfer coefficient (HTC) of the NF. However, the optimal concentration of OA and OAK^+ needs to be determined to maximize the heat transfer rate in the ALT/CV.

Previous research on TPCTs and ALT/CVs has rarely considered NFs containing surfactants and check valves to prevent reverse flows in a tube. Such a valve can control the flow direction and separately manage the liquid and vapor phases. Surfactants can resolve the agglomeration issue and increase the thermal performance of an ALT/CV.

This study evaluated the heat transfer behavior of an ALT/CV filled with an NF containing silver NPs with OA and OAK^+ as surfactants. The effects of the heat input, working fluid, and loop size of the thermosiphon on the thermal behavior (thermal resistance, HTC, and relative thermal efficiency (RTE)) under normal operating conditions were studied. The improved method, working fluid, and cross-sectional tube presented here were developed in previous studies (Parametthanuwat *et al.,* 2015; Bhuwakietkumjohn *et al.,* 2017).

2. Experimental apparatus and procedure

The following equations were used to calculate the heat transfer rate and error analysis and were previously compiled by Bhuwakietkumjohn et al., (2017) (Bhuwakietkumjohn et al., 2017).

2.1. Heat transfer characteristics

The heat transfer performance of a TPCT can be calculated from the ratio of the temperature difference between the evaporator and condenser and the total thermal resistance (Reay *et al.,* 2006):

$$Q_{\text{Theoretical}} = \frac{\Delta T}{Z_{Total}} \tag{1}$$

where

$$\Delta T_{\ln} = \frac{(\mathrm{T_{h,in}} - \mathrm{T_{c,out}}) - (T_{h,\mathrm{out}} - T_{c,in})}{\ln \dfrac{(\mathrm{T_{h,in}} - \mathrm{T_{c,out}})}{(T_{h,\mathrm{out}} - T_{c,in})}} \tag{2}$$

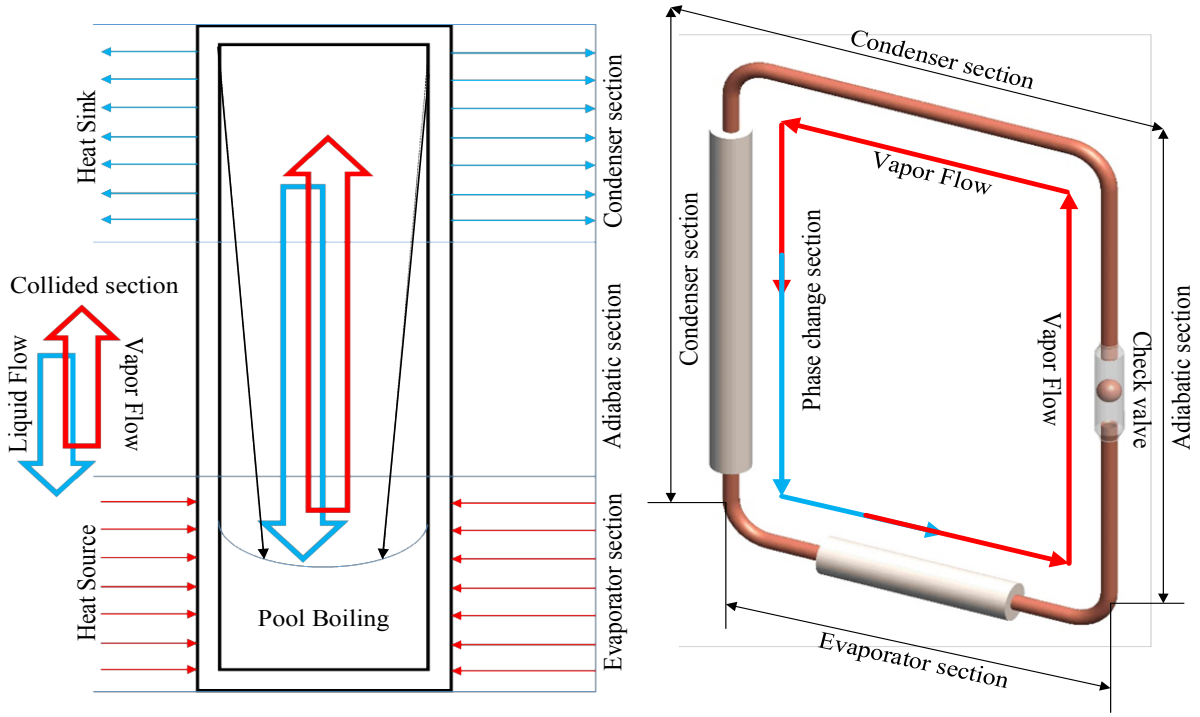

Fig. 1 Schematic of the TPCT and ALT/CV

The total thermal resistance has many factors that depend on the function or properties of the operation. This is represented as the total resistance of the thermal model ESDU 81038 (Anon, 1980).

2.2. Thermal resistance of the thermosiphon

The TPCT is a simple heat transfer device. Its performance can be evaluated according to the total resistance, which is calculated with ESDU 81038 (Anon, 1980). The resistance of a TPCT can be split into ten values that are divided into three groups. The external resistance is the resistance from the outside wall of the TPCT at both the evaporator and condenser. The internal resistance is the resistance from the phase change, pool boiling, or film boiling when the vapor pressure drops along the pipe. The resistance from the material properties depends on the material used. Figure 2 explains the different resistance values (Parametthanuwat *et al.,* 2012).

The external resistances Z_1 and Z_9 are thermal resistance between "heat source and the evaporator external surface" and "heat sink and condenser external surface", respectively. These can be expressed as:

$$Z_1 = \frac{1}{h_{eo} A_{eo}} \tag{3}$$

$$Z_9 = \frac{1}{h_{co} A_{co}} \tag{4}$$

The material property resistances Z_2 and Z_8 are the thermal resistances across the thickness of the thermosyphon tube wall in the "evaporative section" and "condenser section" respectively, which can be determined as

$$Z_2 = \frac{\ln\left(D_o / D_i\right)}{2\pi L_e k_x} \tag{1}$$

$$Z_8 = \frac{\ln\left(D_o / D_i\right)}{2\pi L_c k_x} \tag{2}$$

The internal resistances Z_3 and Z_7 are due to the pool and film boiling of the working fluid and are further divided as follows:

- Z_{3p} is the resistance from pool boiling:

$$\frac{1}{\Phi_3 g^{0.2} Q^{0.4} \left(\pi D_i L_e\right)^{0.6}} \tag{7}$$

- Z_{3f} is the resistance from film boiling at the evaporator:

$$\frac{CQ^{1/3}}{D_i^{4/3} g^{1/3} L_e \Phi_2^{4/3}} \tag{8}$$

Where $C = \left(\frac{1}{4}\right)\left(\frac{3}{\pi}\right)^{4/3} = 0.325$,

- Φ_2 is the figure of merit as $\left(\frac{L k_l^3 \rho_l^3}{\mu_l}\right)^{0.25}$ for case of film boiling,
- Φ_3 is the figure of merit as $0.325 \times \frac{\rho_l^{0.5} k_l^{0.3} C_{pl}^{0.7}}{\rho_v^{0.25} L^{0.4} \mu_l^{0.1}} \left[\frac{P_v}{P_a}\right]^{0.23}$ for nucleate boiling.

Z_{3p} and Z_{3f} can be combined into $Z_3 = Z3pF + Z3f\left(1-F\right)$ where F is the filling ratio and is defined by $\frac{V_l}{AL_e}$. Z_7 is the resistance from film boiling of the working fluid at the condenser:

$$Z_7 = \frac{CQ^{1/3}}{D_i^{4/3} g^{1/3} L_c \Phi_2^{4/3}} \tag{9}$$

Z_7 and Z_6 are the resistances due to phase changes at the evaporator and condenser, respectively. Z_5 is the resistance due to the pressure drop along the pipe. Z_{10} is the resistance due to heat conduction along the axial pipe. Normally, Z_4, Z_5, Z_7 and Z_{10} have small values and can be neglected. Thus, Z_{Total} can be defined as follows:

$$Z_{Total} = Z_1 + \left[\begin{matrix}(Z_2 + Z_3 + Z_4 + Z_5 + \\ Z_6 + Z_7 + Z_8)^{-1} + (Z_{10})^{-1}\end{matrix}\right]^{-1} + Z_9 \tag{10}$$

However, the ALT/CV is analogous to a TPCT with the evaporator, adiabatic, and condenser sections arranged in a rectangular tube. This body shape can be defined by the outside tangent line of the ALT/CV, as shown in Figure 2. The ALT/CV is defined by the constant proportionality reciprocal to the thermal resistance Z_{Total}. The ALT/CV should improve the pool boiling, which affects the heat transfer performance and behavior. Table 1 describes the experimental parameters used in this study. In total, there were 2430 experimental parameters (5 × 3 × 3 × 3 × 3 × 6).

The experiment was repeated threefold. NFs were prepared with deionized (DI) water as the base fluid. The NPs (silver nanopowder with a particle size of <100 nm and metal basis of 99.9%), OA, and OAK^+ were purchased from Sigma-Aldrich, Inc. (USA). NFs were obtained using a sonicator (bath type; operating frequency, 43 kHz; and power source, AC100–120 V/AC220–240 V at 50/60 Hz) to apply ultrasonic vibrations for 12 h. The silver NPs were suspended in DI water at a concentration of 0.5 wt%. Then, OA and OAK^+ were added to the NF at concentrations of 0.5, 1, and 1.5 wt%.

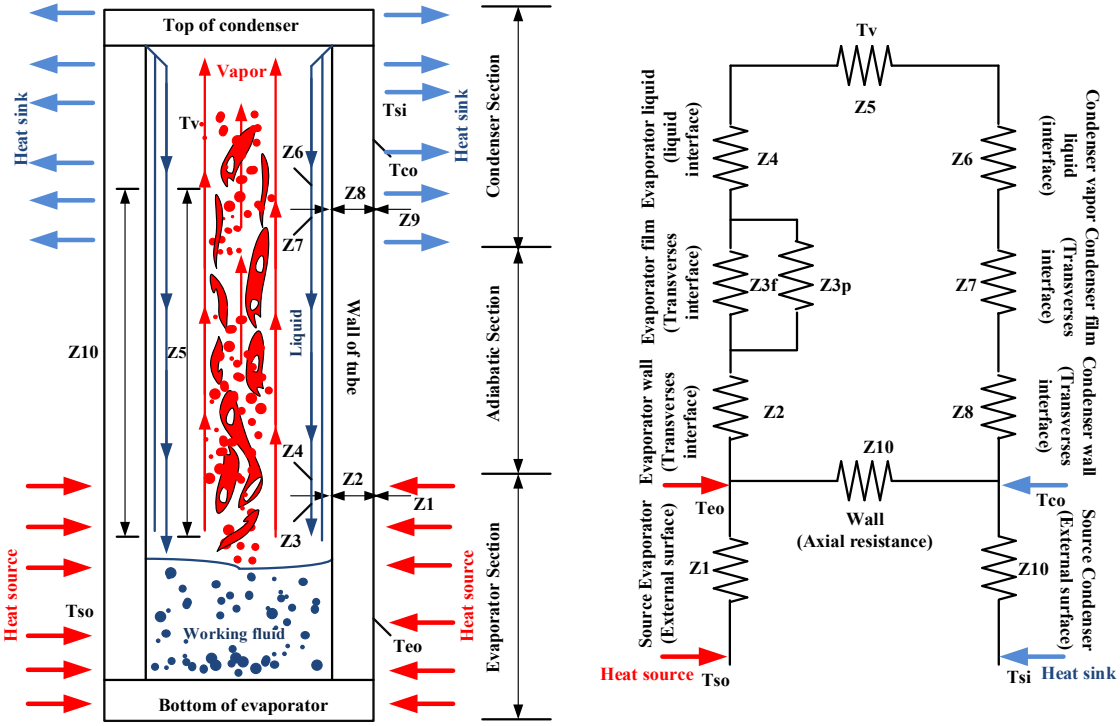

Fig. 2 Model for the total resistance of the TPCT according to ESDU 81038 (Anon., 1980)

Table 1
Controlled and variable parameters for the ALT/CV thermal performance and behavior

Controlled parameters	• The ALT/CV was made from a copper tube with an inside diameter of 12.70 mm. • The temperature of the cooling fresh air was 25°C. • The ambient temperature was 25°C. • The air velocity at the condenser inlet was 0.6 m/s.

Independent variables	• The heat supply was 20%, 40%, 60%, 80%, and 100% of the heater capacity (2000 W).
	• The filling ratio was 30%, 50%, and 80% with respect to the evaporator volume.
	• The ALT/CV was a loop with three sections: an evaporator, adiabatic section, and condenser. Three loop sizes were considered: 30, 40, and 50 cm, respectively. Fins were installed at a fin density of 8 FPI in the condenser.
	• Working fluids:
	  ○ Deionized (DI) water
	  ○ DI water containing surfactant
	  ○ NF
	  ○ NF containing surfactant
	• Surfactants:
	  ○ 0.5, 1, and 1.5 wt% OA
	  ○ 0.5, 1, and 1.5 wt% OAK^+

Dependent variables	• Heat transfer rate (W) • Heat flux (W/m^2) • Thermal resistance (W/°C)

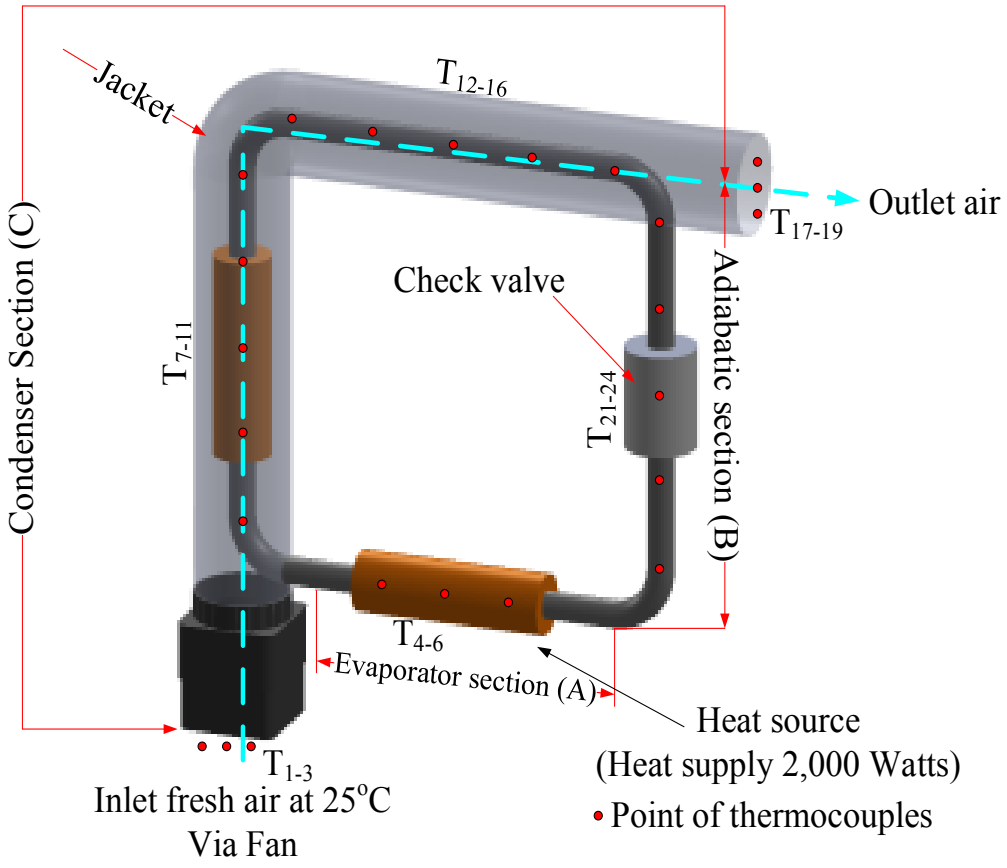

Fig. 3 Schematic diagram of the experimental apparatus

Figure 3 shows a schematic diagram of the experimental apparatus, which consisted of an ALT/CV. The evaporator (Section A) was the heat source with a heat supply of 2000 W. The adiabatic section (Section B) was not involved in the heat transfer and connected the other two sections. The condenser (Section C) was the heat sink and was supplied with fresh air (controlled at 25°C). The ALT/CV was made from copper tubes with an internal diameter of 12.70 mm. The evaporator, adiabatic section, and condenser comprised a loop. Three loop sizes were considered: 30, 40, and 50 cm. Fins were installed in the condenser at a fin density of 8 FPI. The temperature was measured at 24 points in the adiabatic section with K-type thermocouples (OMEGA with ±0.1°C accuracy). The thermocouples were installed along with a data logger attached to the ALT/CV (Yokogawa DX200 with an accuracy of ±0.1°C, 24-channel input, and range of −200 to 1,100°C) at the positions indicated by circles in Figure 3. The jacket was covered with insulation. The flow and velocity of the fresh air were controlled with an AC motor. Table 1 shows the controlled and variable parameters.

During the experiment, the air velocity was set to 0.6 m/s (25°C), and the calorific method was used to calculate the heat transfer characteristics of the ALT/CV. The following equations were used to calculate the heat transfer rate and for the error analysis (O'Hanley *et al.*, 2012):

$$Q_{Experimental} = \dot{m} C_p (T_{out} - T_{in}) \quad (3)$$

where

$$Q = f(\dot{m}, T_{out}, T_{in}) \quad (4)$$

The error analysis of the heat transfer was based on the following (Parametthanuwat *et al.*, 2011):

$$Q = \left[\left(\frac{\partial Q}{\partial \dot{m}} \times \dot{m} \right)^2 + \left(\frac{\partial Q}{\partial T_{out}} \times T_{out} \right)^2 + \left(\frac{\partial Q}{\partial T_{in}} \times T_{in} \right)^2 \right]^{0.5} \quad (5)$$

3. Results and Discussion

3.1 Temperature distribution of the ALT/CV

Fig shows the adiabatic temperature at the upper part and side of the ALT/CV over time. The temperature increased with time. The maximum temperature difference between T_{inlet} and T_{outlet} was ±5°C and was achieved with the NF of 0.5 wt% silver NPs and 1 wt% OAK^+ and operating percentage of the heat supply (OPHS) of 100%. T_{inlet} was higher than T_{outlet} causing higher thermal performance. The adiabatic temperature became higher than the ambient temperature, so heat transfer occurred. The working fluid and position of the heat source affected the thermal performance (Faghri, 1995). The heat transfer was in the transient state from the start of the experiment to 400 s and then showed a steady state from

that point. The transient state of the heat transfer was because of the unequal vapor and liquid phases of the working fluid flowing in the loop and passing through the check valve of the thermosiphon, which resulted in a nonuniform temperature distribution. The steady state was achieved when the ball in check valve moved through the saturated and superheated vapor and experienced a force in the direction opposite to its motion. The terminal velocity was achieved when the drag force was equal in magnitude but opposite in direction to the force propelling the object. The effect of ball buoyancy was evaluated as follows. The ball moved in the upward direction when the forces satisfied the following condition:

$$\frac{F_{upward}}{A_{ball}} > \frac{(-\mathrm{F}_{\tau} - F_{\sigma} - \mathrm{F}_{\mathrm{g}} + \mathrm{F}_{\mathrm{d}})_{\mathrm{ball}}}{A_{ball}} \tag{6}$$

The ball moved in the downward direction when the forces satisfied the following condition:

$$\frac{F_{downward}}{A_{ball}} < \frac{(\mathrm{F}_{\tau} + F_{\sigma} + \mathrm{F}_{\mathrm{g}} - \mathrm{F}_{\mathrm{d}})_{\mathrm{ball}}}{A_{ball}} \tag{7}$$

The force direction due to the pressure difference $(\Delta \mathrm{P})$ occurred when the flow was separated into vapor and liquid. This relation defined the heat transfer mechanism that generated pressure in the evaporator. In this case, $P_{upward} \geq F_{ball\,total}$ caused the ball buoyancy to affect T_{inlet} and T_{outlet} when there was a temperature difference $(\Delta \mathrm{T})$. Consequently, the check valve of the ALT/CV could regulate and control $\Delta P \infty \Delta T$, as shown in Figure 5.

3.2 Effect of the operating percentage of the heat supply

Figure 6 shows the heat transfer of the ALT/CV at a loop size of 50 cm as a function of the OPHS. There were 14 working fluids that were considered. The data shown correspond to a filling ratio of 50% of the evaporator volume. The results indicate that the NF of 0.5 wt% silver NPs and 1 wt% OAK+ produced a heat transfer rate of 1150 W at an OPHS of 100%. Then, all of the experimental data were compared to the heat transfer rate of the ALT/CV without the working fluid or base fluid. In all cases, the NF of 0.5 wt% silver NPs and 1 wt% OAK+ showed a superior heat transfer rate over all experimental conditions. For a given working fluid, the heat transfer rate increased with the OPHS, which confirms that the OPHS had a strong effect on the heat transfer rate and working fluid properties. The peak heat transfer rate occurred at an OPHS of 100%. The viscosity and surface tension decreased when OA and K+ were introduced (Bhuwakietkumjohn *et al*., 2017; Hwang *et al.,* 2008). The viscosity and surface tension of the working fluids decreased as the operating temperature increased, which made the working fluid easier to boil. Introducing OA allowed the NPs to uniformly disperse within the base fluid. A high OA concentration appeared to hinder the aggregation of the NPs, which was observed at the bottom of the liquid (Li *et al*., 2008; Sharma *et al.,* 2011; Warrier *et al.,* 2011). These experimental results for the heat transfer rate agree with those in the literature (Hwang *et al*., 2008; Sharma *et al*., 2011; Li *et al.,* 2008). In this study, the optimal OAK+ concentration for the NF was 1 wt%, which led to the highest heat transfer rate under all conditions.

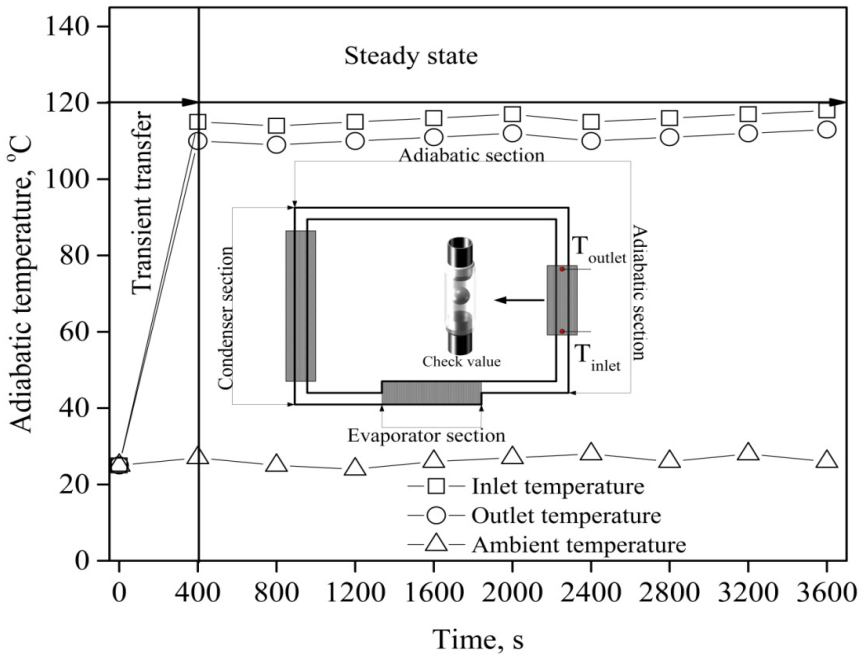

Fig 4 Temperature distribution of loop thermosyphon in the adiabatic section

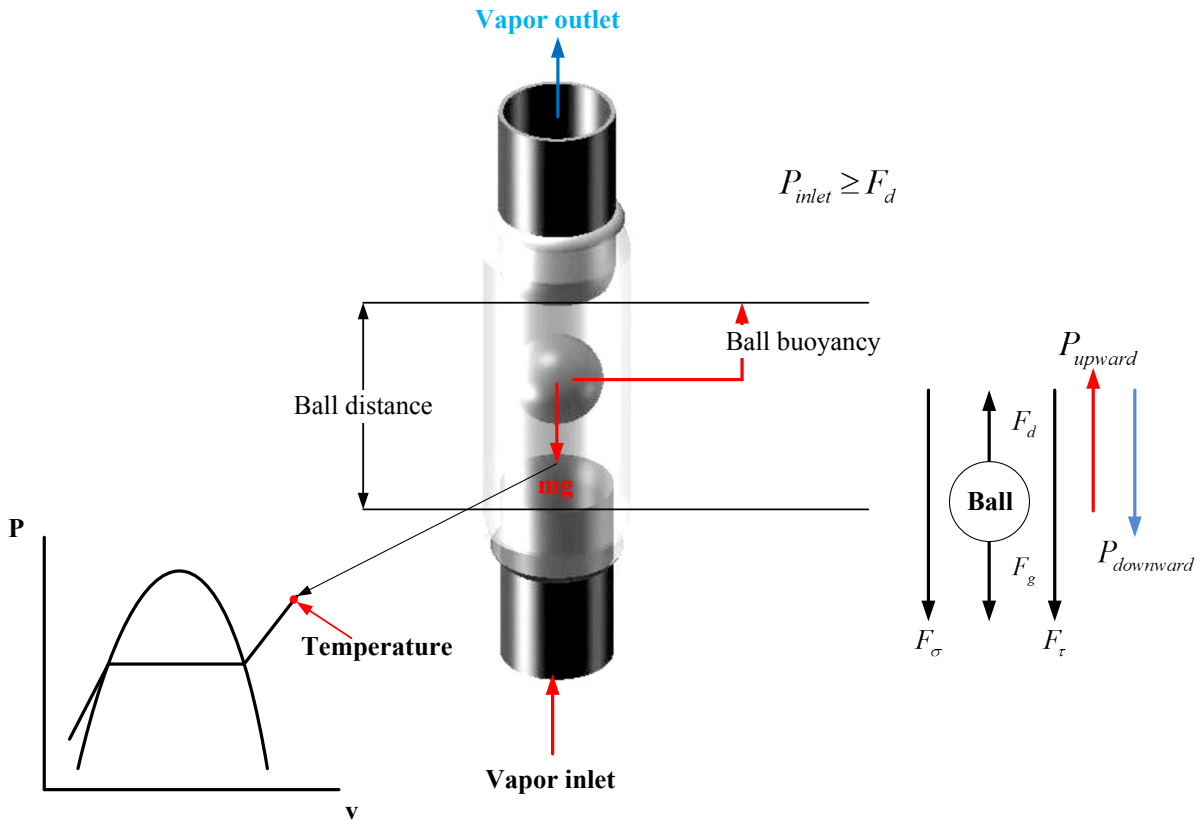

Fig. 5 Check valve operation

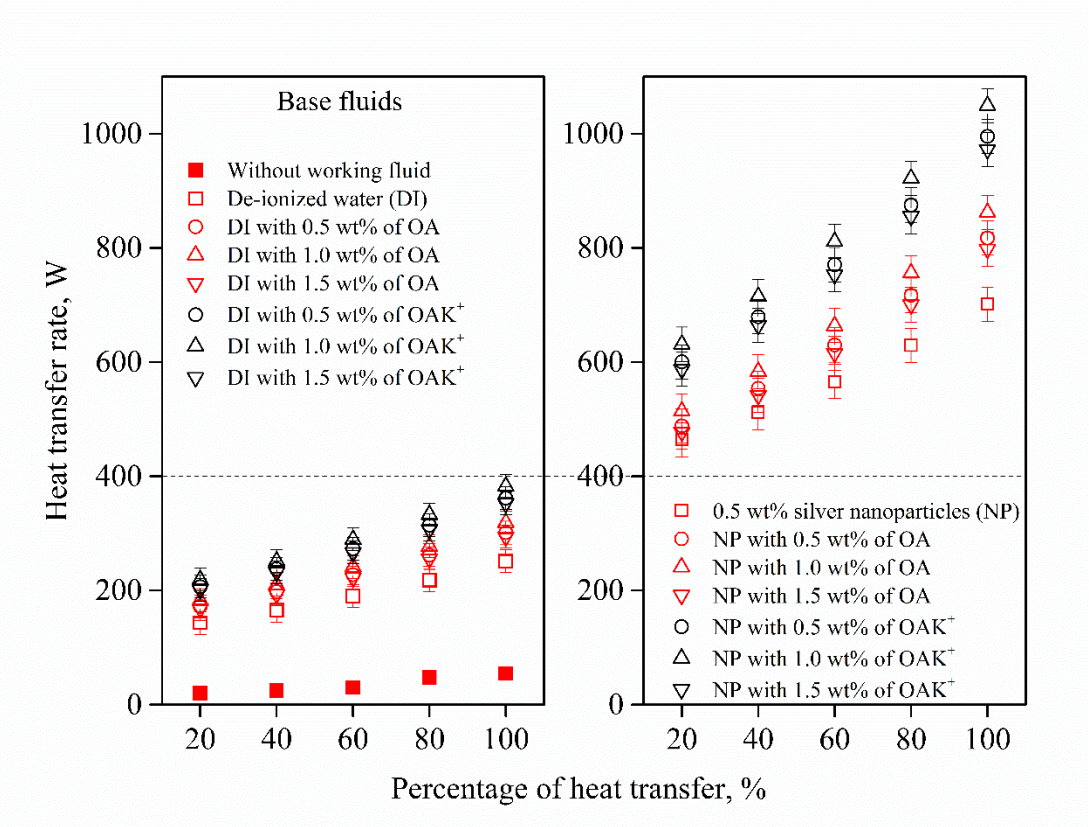

Fig. 6 Effect of the operating percentage of heat supplied

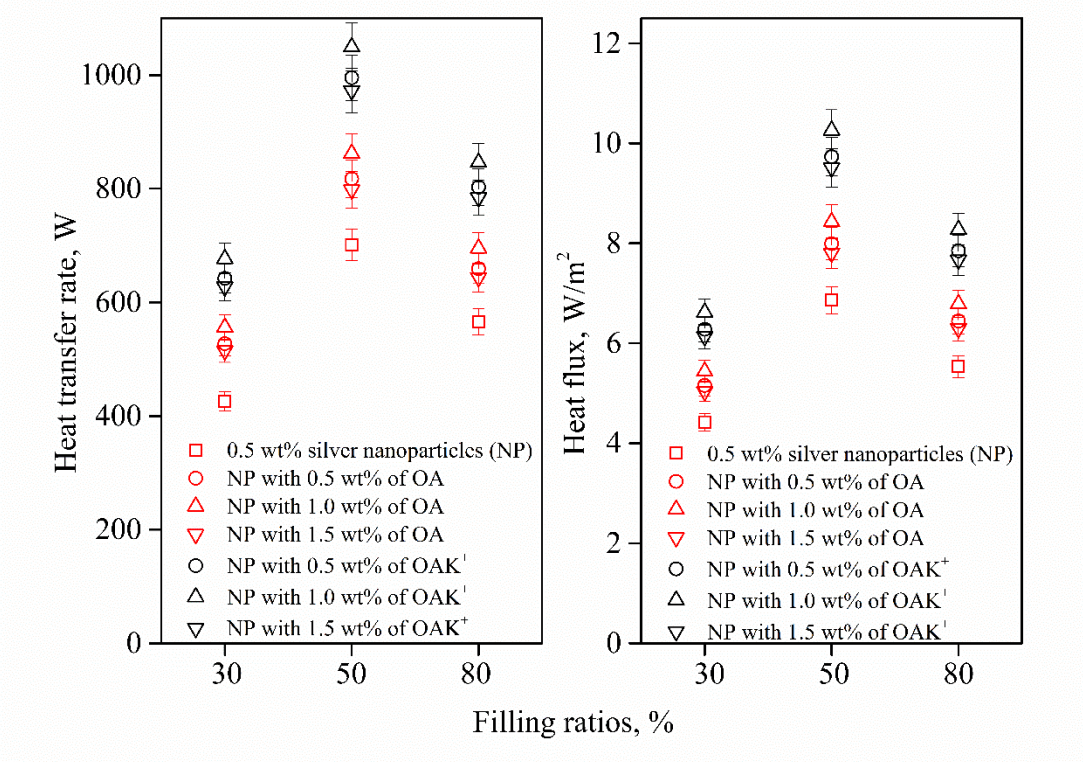

Fig. 7 Effect of the filling ratio of the working fluid

3.3 Effect of the loop size of the thermosiphon

Figure 8 shows the heat transfer rate and heat flux according to the loop size of the thermosiphon. The experimental results clearly indicated that the maximum heat transfer rate of 1150 W was achieved with the NF of 0.5 wt% silver NPs and 1 wt% OAK$^+$ at a loop size of 50 cm and OPHS of 100%. This heat transfer rate was greater than that achieved by Paramatthanuwat *et al.* (2010) for a TPCT and by Bhuwakietkumjohn *et al.* (2017) for a rectangular TPCT. However, the current experimental results do not agree with those of the two studies. Thus, the vast differences among different experimental conditions must be acknowledged, especially with regard to the type of heat pipe and thermosiphon. When the loop size was increased from 30 to 50 cm, the heat transfer rate only slightly increased. The increase in the loop size is equivalent to increasing the size of the evaporator for the ALT/CV. A larger evaporator increases pool boiling, which increases the heat transfer rate. The small aspect ratio leads to boiling in the confined channel, which reduces the heat transfer rate (Lock, 1992; Paramatthanuwat *et al.,* 2010). Changing the loop size affected the filling ratio, which in turn affected the heat transfer rate (Khandekar *et al.,* 2008). The silver NPs were very small, so adding surfactants uniformly dispersed the NPs in the fluid. This increased the surface area of bubbles for absorbing heat (Bhuwakietkumjohn *et al.,* 2010; Terdtoon *et al.,* 1998), which facilitated boiling of the fluid. This led to a high amount of condensate that could return to the evaporator section, which ensured an ample amount of working fluid for boiling and phase transition to occur (Hwang *et al.,* 2008; Kwak *et al.,* 2005; Lin *et al.,* 2008).

3.4 Effect of the thermal resistance

The thermal resistance affects the pool boiling/film boiling in the evaporator section, and it can be estimated according to ESDU 81038 (Anon, 1980). Adding surfactants to the NF increases the surface tension and decreases the wettability of the NPs but results in increased thermal properties for the thermosiphon (Solomon *et al.,* 2013; Parametthanuwat *et al.,* 2015). The boiling phenomenon can be explained according to the thermal/physical properties of the working fluid and physical properties of the thermosiphon, which are important for thermal resistance. Changing the cross section causes friction loss and affects the phase transfer, which reduces film boiling (Bhuwakietkumjohn *et al.,* 2017). However, Figure 9 shows that the current experimental results contrast with those of other studies (Noie-Baghban, 2005; Bhuwakietkumjohn *et al.,* 2017; Imura *et al.,* 1977; Srimuang *et al.,* 2009; Amtachaya, 2010). In the present study, the results were obtained with a different heat source, working fluid, and conditions compared with those used in the other studies. The minimum thermal resistance was 4.76×10^{-4} °C/W for a loop size of 50 cm and NF of 0.5 wt% silver NPs and 1 wt% OAK$^+$. Increasing the loop size of the thermosiphon decreased the thermal resistance. The thermal resistance increased with the OPHS because the ALT/CV was a single loop. The other studies in Figure 9 evaluated different kinds of thermosiphons under different conditions. The type of thermosiphon affects boiling phenomena. Pool boiling generally occurs with a low thermal resistance, which requires a high thermal performance. Pool boiling can also occur inside a confined channel, which has high thermal resistance. The original

TPCT in Figure 2 had a higher thermal resistance than the ALT/CV because of the differences in the cross section and section where the vapor and liquid phases collide. The TPCT generated a larger pressure drop (ΔP) in the condenser section. Figure 1 shows that the ALT/CV changes the cross section and collided section. The dose was reduced by the check valve but was eliminated by the loop cross section of the ALT/CV in the condenser and adiabatic section. The ALT/CV helped separate the collided section, which may improve the heat transfer due to phase change and affect the heat transfer behavior. The check valve controlled the pressure drop (ΔP) and amount of working fluid phase, which decreased condensation in the condenser. The check valve increased pool boiling by controlling the amount of working fluid, which reduced flooding in the evaporator.

3.5. Effect of the heat transfer coefficient

Figure 10 shows the HTC for an ALT/CV with a loop size of 50 cm and OPHS of 100%. At a filling ratio of 50%, the samples showed similar positive trends. The HTC depended on the filling ratio and surfactant concentration. In all cases at a filling ratio of 50%, the NF of 0.5 wt% silver NPs and 1 wt% OAK^+ showed a superior performance compared to the other working fluids. The NF of 0.5 wt% silver NPs and 1 wt% OAK^+ had the highest HTC of 20,986.029 W/m^2 K. The HTC seemed to have an inverse relationship with the thermal resistance (Lock, 1992; Yu *et al.,* 2007). This is because the filling ratio and surfactant concentration increase with the viscosity of the working fluid, which results in the movement of the NPs. Brownian motion leads to greater dispersion of the NPs inside the NF, which in turn increases the convection transfer. This remarkably increases convection-like effects, which increases the HTC (Li, 2002; Zamzamian *et al.,* 2011). For all working fluids, the HTC increased with the OPHS. These experimental results are comparable with those in the literature (Noie-Baghban, 2005; Bhuwakietkumjohn *et al.,* 2017; Imura *et al.,* 1977; Srimuang *et al.,* 2009; Lee *et al.,* 2003). The HTC of the ALT/CV showed a linear dependance on the OPHS for all samples, which indicates that the HTC increased according to the surfactant concentration. The HTCs of the NFs containing surfactant differed at surfactant concentration of 0.5, 1, and 1.5 wt%. In all cases, the DI water containing surfactant and NF with OAK^+ showed superior performance than the base fluid. However, the HTC was higher than those reported by the above five studies because the check valve of the ALT/CV separately controlled the liquid and vapor phases. This may have increased the pool boiling in the evaporator and condensation in the condenser section. Hence, the HTC depended on the heat transfer due to phase change. Moreover, the NPs dispersed in the NF increase the surface area for heat absorption. For the NF containing OAK^+, the surfactant decreased the surface tension and stabilized the NF by uniformly distributing NPs while increasing the interface area with the DI water (Jiao *et al.,* 2008). The surface tension has a significant influence on the thermal process because it depends on the properties and interfacial equilibrium (Ramesh *et al.,* 2011). A high OAK^+ concentration appeared to hinder aggregation, and entanglement of the NPs was observed at the bottom of the liquid (Li *et al.,* 2008; Sharma *et al.,* 2011). The experimental results of the present study indicated that 1 wt% OAK^+ was sufficient to realize the homogeneous dispersion of NPs and efficient thermal transfer between the particles and DI water. This consequently maximized the thermal properties (Buongiorno *et al.,* 2009; Godson *et al.,* 2010; Kang *et al.,* 2009; Patel *et al.,* 2003). The NF was dominated by pool boiling because of the large amount of heat transfer inside the ALT/CV.

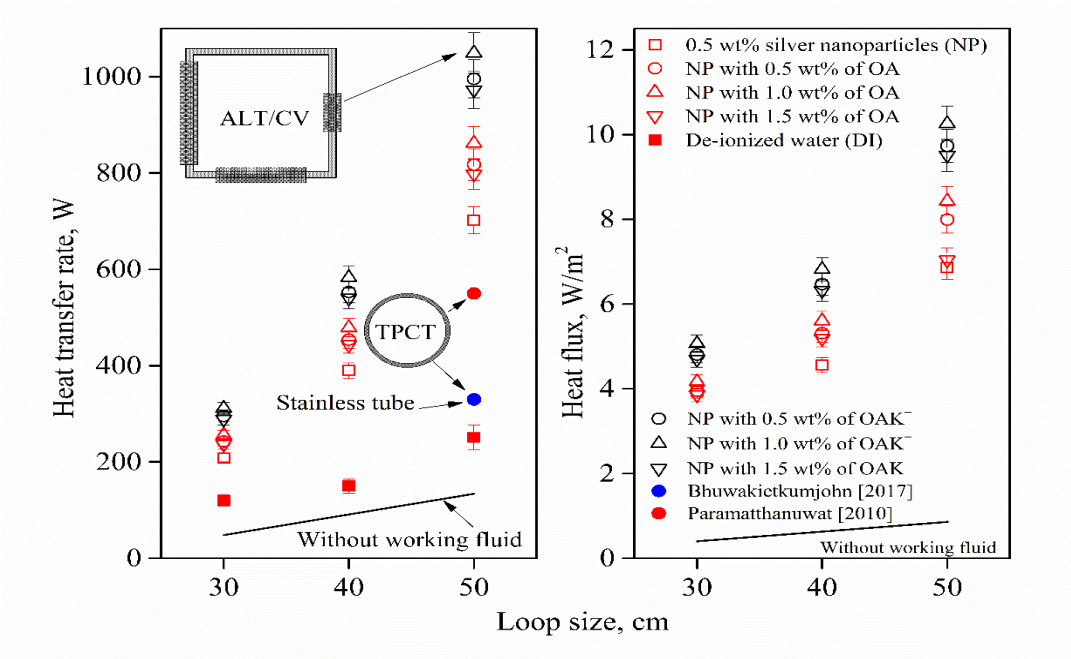

Fig. 8 Effect of the loop size of the thermosiphon

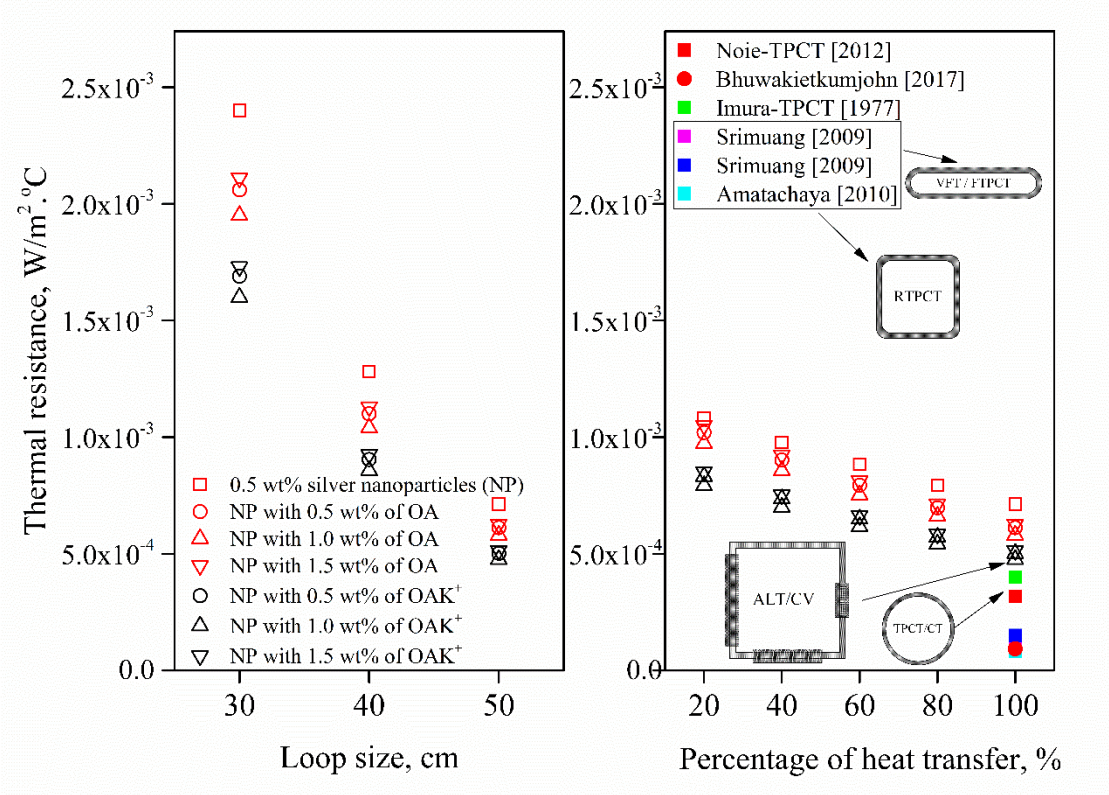

Fig. 9 Effect of the thermal resistance

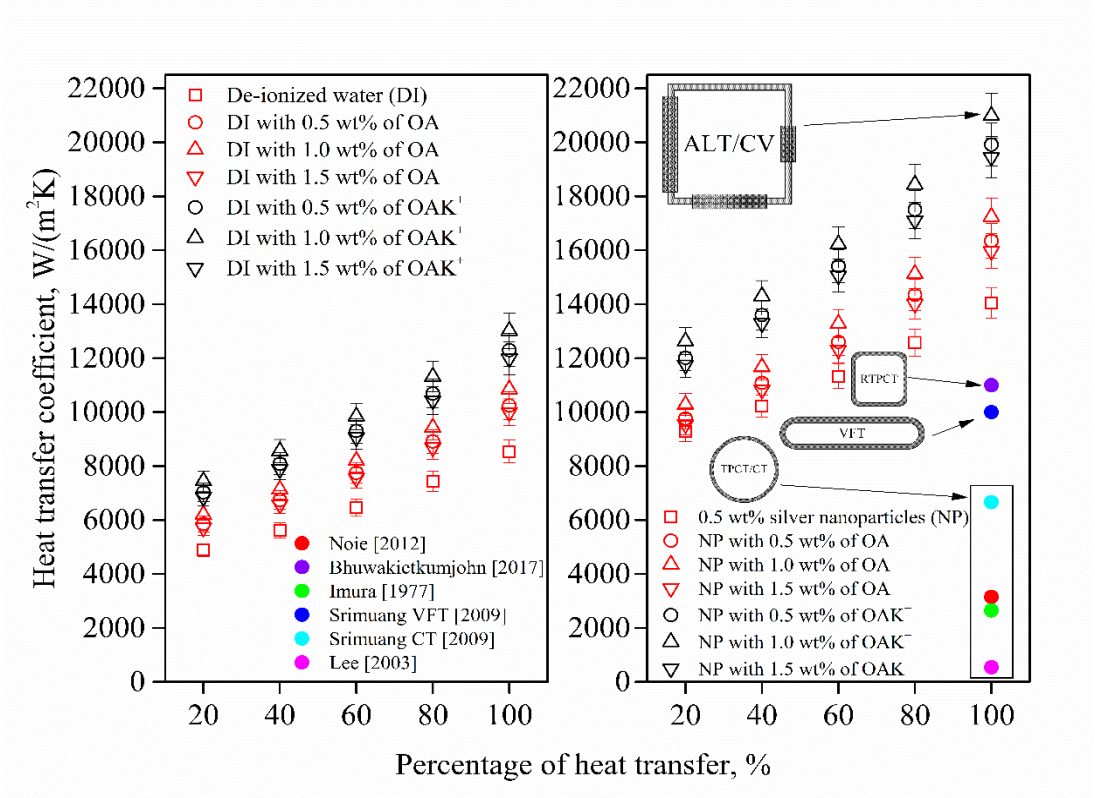

Fig. 10 Effect of the heat transfer coefficient

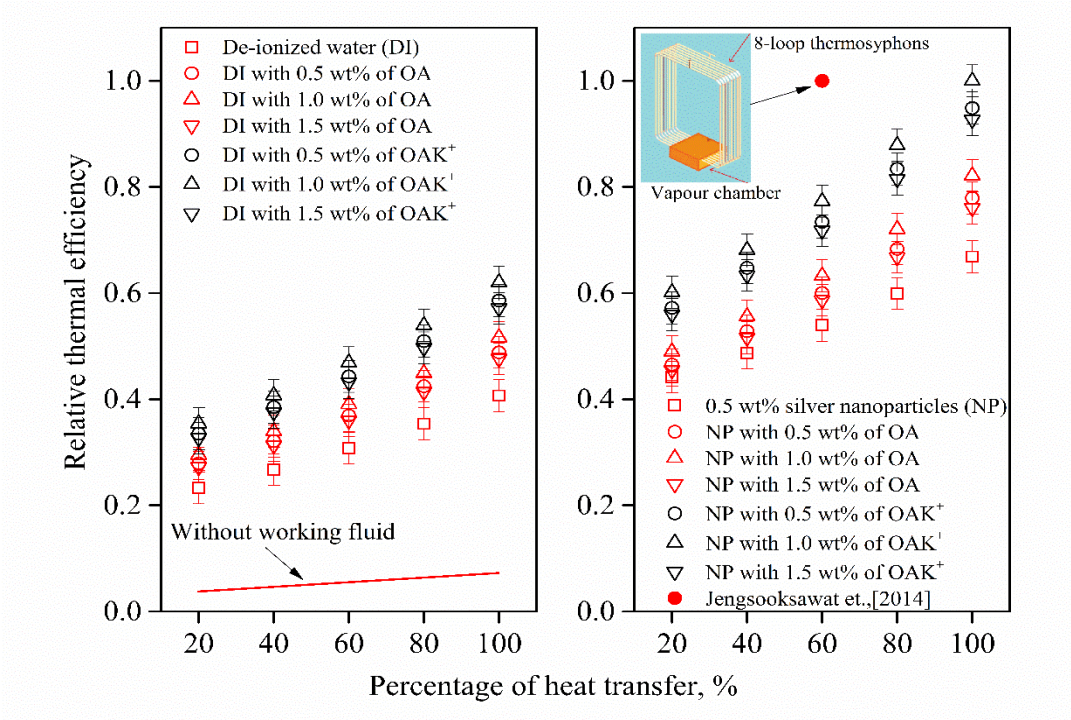

Fig. 11 Effect of the relative thermal efficiency

3.6. Effect of the relative thermal efficiency

Figure 11 shows the RTE of all working fluids in this study for a loop size of 50 cm, filling ratio of 50%, and OPHS of 100%. The maximum RTE was achieved with 1 wt% OAK+. The check valve maximized the heat transfer because it separated and controlled the flow of the liquid and vapor phases (Dangeton *et al.,* 2012; Rittidech *et al.,* 2007; Rittidech *et al.,* 2012). However, the current experimental results do not agree with those of Jengsooksawat *et al.* (2014), who used an eight-loop thermosiphon with an 100% OPHS of 1200 W, air velocity of 0.5 m/s, filling ratio of 60%, and ethanol as the working fluid. Thus, the differences in experimental conditions must be acknowledged, especially with regard to the type of heat pipe and thermosiphon. The motion of the NPs enhanced the thermal conductivity of the NF. OAK+ helped facilitate the homogeneous dispersion of the NPs in the NF. Brownian motion significantly increased the thermal conductivity of the NF, which is a more efficient heat transfer mechanism than thermal diffusion (Kwak & Kim, 2005; Patel *et al.,* 2003).

4. Conclusion

This study evaluated the thermal behavior of an ALT/CV, with a particular focus on the effect of the check valve. The following conclusions were obtained:

- The ALT/CV with a loop size of 50 cm showed the best heat transfer behavior at a filling ratio of 50% and OPHS of 100% when the working fluid was a NF of 0.5 wt% silver NPs and 1 wt% OAK+. The loop size of 50 cm and filling ratio of 50% yielded the optimal thermal behavior among all experimental conditions considered in this study with an RTE of about 1.
- The ALT/CV reduced the pressure drop (ΔP), which was insignificant in the evaporator and condenser. This increased the pool boiling and condensation phenomena, which improved the heat transfer performance compared to the original TPCT.

The ALT/CV provides a better thermal performance than the conventional thermosiphon. The loop-type thermosiphon with a check valve is suitable for applications in heat transfer engineering. The presence of a surfactant such as OAK+ clearly improves the heat transfer rate and NF properties.

Nomenclature

A_{ball}	Surface area of the ball	m²
C_p	Specific heat capacity constant	kJ/kg·°C
C_{pl}	Specific heat capacity of the working fluid in the liquid phase	kJ/kg·°C
D_o	Outside diameter of the pipe	m
D_i	Inside diameter of the pipe	m
F	Force	N
g	Gravity	m/s²
h_e	Heat transfer coefficient	W/m²

h	Latent heat of vaporization	kJ/kg
k_x	Thermal conductivity of the material	W/°C·m
k_l	Thermal conductivity of the working fluid in the liquid phase	W/°C·m
L	Characteristic length	m
$\dot{m}$	Mass flow rate	kg/s
NP	0.5 wtsilver nanoparticles % in DI water	
OA	Oleic acid	
OAK^+	Potassium oleate	
P_v	Vapor pressure of the working fluid	Pa
P_a	Atmospheric pressure (101.3 kPa)	
P_{upward}	Upward pressure	Pa
Q	Heat transfer rate	W
$Q_{Theoretical}$	Theoretical heat transfer rate	W
$Q_{Experimental}$	Experimental heat transfer rate	W
$T_{h,in}$	Inlet temperature for the evaporator	°C
$T_{h,\text{out}}$	Outlet temperature for the evaporator	°C
$T_{\text{c},in}$	Inlet temperature for the condenser	°C
$T_{\text{c,out}}$	Outlet temperature for the condenser	°C
Z_{total}	Total thermal resistance	W/m² ·°C
ρ_l	Density of the working fluid in the liquid phase	kg/m³
ρ_v	Density of the working fluid in the vapor phase	kg/m³
μ_l	Viscosity of the working fluid in the liquid phase	N/m
ν	Momentum diffusivity (kinematic viscosity)	m²/s
σ	Surface tension	N/m

Acknowledgment

T. Parametthanuwat is from the Faculty of Industrial Technology and Management at King Mongkut's University of Technology North Bangkok and was financially supported by King Mongkut's University of Technology North Bangkok via Grant No. KMUTNB–GEN–59–48. S. Rittidech is the Head of the Heat Pipe and Thermal Tool Design Research Unit (HTDR), Faculty of Engineering, Mahasarakham University, Thailand. Y. Ding is from the Centre for Thermal Energy Storage School of Chemical Engineering, University of Birmingham, UK. Technical support was provided by N. Bhuwakietkunjohn.

References

Amtachaya W., P. and S. (2010). Comparative heat transfer characteristics of a flat two-phase closed thermosyphon (FTPCT) and a conventional two-phase closed thermosyphon (CTPCT). *Heat and Mass Transfer,* 37, 293–298.

Anon. (1980). Heat pipes-general information on their use, operation and design, Data Item No. 80013..ciences Data Unit.

Bhuwakietkumjohn, N., & Parametthanuwat, T. (2015). Application of silver nanoparticles contained in ethanol as a working fluid in an oscillating heat pipe with a check valve (CLOHP/CV): a thermodynamic behavior study. *Heat and Mass Transfer,* 51, 1219–1228.

Bhuwakietkumjohn, N., & Parametthanuwat, T. (2017). Heat transfer behavior of silver particles containing oleic acid surfactant: application in a two phase closed rectangular cross sectional thermosyphon (RTPTC). *Heat and Mass Transfer*, 53, 37–48

Bhuwakietkumjohn, N., & Rittidech, S. (2010). Internal flow patterns on heat transfer characteristics of a closed-loop oscillating heat-pipe with check valves using ethanol and a silver nano-ethanol mixture. *Experimental Thermal and Fluid Science,* 34(8), 1000–1007.

Brusly Solomon, A., Mathew, A., Ramachandran, K., Pillai, B. C., & Karthikeyan, V. K. (2013). Thermal performance of anodized two phase closed thermosyphon (TPCT). *Experimental Thermal and Fluid Science*, 48, 49–57.

Buongiorno, J., Venerus, D. C., Prabhat, N., McKrell, T., Townsend, J., Christianson, R., Tolmachev, Y. V, Keblinski, P., Hu, L., Alvarado, J. L., Bang, I. C., Bishnoi, S. W., Bonetti, M., Botz, F., Cecere, A., Chang, Y., Chen, G., Chen, H., Chung, S. J., … Zhou, S.-Q. (2009). A benchmark study on the thermal conductivity of nanofluids. *Journal of Applied Physics*, 106(9).

Chen, H., Ding, Y., & Tan, C. (2007). Rheological behavior of nanofluids. New Journal of Physics, 9 367

Choi J.A., S. U. S. and E. (1995). Enhancing thermal conductivity of fluids with nano-particles. Int. Mech. Eng. Congr. Exhib.

Dangeton, W., Pattiya, A., Rittidech, S., & Siriwan, N. (2012). Flow Visualization of a Miniature Loop Thermosyphon. *Experimental Heat Transfer,* 26(4), 329–342.

Faghri, A. (1995). Heat Pipe Science and Technology (1st ed.). Taylor&Francis.

Godson, L., Raja, B., Lal, D. M., & Wongwises, S. (2010). Experimental Investigation on the Thermal Conductivity and Viscosity of Silver-Deionized Water Nanofluid. E*xperimental Heat Transfer,* 23(4), 317–332.

Hwang, Y., Lee, J. K., Lee, J. K., Jeong, Y. M., Cheong, S. I., Ahn, Y. C., & Kim, S. H. (2008). Production and dispersion stability of nanoparticles in nanofluids. *Powder Technology,* 186(2), 145–153.

Imura, H., Kusada, H., Oyata, J., Miyazaki, T., & Sakamoto, N. (1977). Heat transfer in two-phase closed-type thermosyphons. Transactions of Japan Society of Mechanical Engineers, 22, 485–493.

Jengsooksawat, S., Booddachan, K., & Rittidech, S. (2014). Loop Thermosyphon with Vapour Chamber : A Thermodynamic Study. *Advances in Mechanical Engineering*, 6, 1–8.

Jengsooksawat, S., Pimpru, S., Booddachan, K., & Rittidech, S. (2008). Heat Transfer Characteristic of Loop Thermosyphon with Vapor Chamber. In The 9th International Heat pipe Symposium (pp. 215–218).

Jiao, B., Qiu, L. M., Zhang, X. B., & Zhang, Y. (2008). Investigation on the effect of filling ratio on the steady-state heat transfer performance of a vertical two-phase closed thermosyphon. *Applied Thermal Engineering*, 28, 1417–1426.

Kang, S. W., Wei, W. C., Tsai, S. H., & Huang, C. C. (2009). Experimental investigation of nanofluids on sintered heat pipe thermal performance. *Applied Thermal Engineering,* 29(5–6), 973–979.

Khandekar, S., Joshi, Y. M., & Mehta, B. (2008). Thermal performance of closed two-phase thermosyphon using nanofluids. *Thermal Science,* 47, 667–695.

Kwak, K., & Kim, C. (2005). Viscosity and thermal conductivity of copper oxide nanofluid dispersed in ethylene glycol. *Korea-Australia Rheology Journal*, 17(2), 35–40.

Lee, J. S., Rhi, S. H., Kim, C. N., & Lee, Y. (2003). Use of two-phase loop thermosyphons for thermoelectric refrigeration: experiment and analysis. *Applied Thermal Engineering*, 23(9), 1167–1176.

Li, X. F., Zhu, D. S., Wang, X. J., Wang, N., Gao, J. W., & Li, H. (2008). Thermal conductivity enhancement dependent pH

and chemical surfactant for Cu-H2O nanofluids. *Thermochimica Acta*, 469(1–2), 98–103.

Li, Z. H. (2002). Modeling and optimization for heat exchanger networks synthesis based on expert system and genetic algorithm. *Chinese Journal of Chemical Engineering*, 10(3), 290–297.

Lin, Y. H., Kang, S. W., & Chen, H. L. (2008). Effect of silver nano-fluid on pulsating heat pipe thermal performance. *Appl Ther Eng,* 28, 1312–1317.

Lock, G. S. H. (1992). The tubular thermosyphon variations on a theme (1st (ed.)). Oxford University Press.

Mahbubul, I. M. (2019). Rheological Behavior of Nanofluid. In Preparation, Characterization, Properties and Application of Nanofluid, 1st, William Andrew, Oxford

Michaelides, E. E., & Ding, Y. (2016). Nanofluids. In Multiphase Flow Handbook, 2nd Edition, CRC Press, Boca Raton

Noie-Baghban, S. H. (2005). Heat transfer characteristics of a two phase closed thermosyphon. *Applied Thermal Engineering*, 25, 495–506.

Noie, S. H., Emami, M. R. S., & Khoshnoodi, M. (2007). Effect of inclination angle and filling ratio on thermal performance of a two-phase closed thermosyphon under normal operating conditions. *Heat Transfer Engineering*, 28(4), 365-371

O'Hanley, H., Buongiorno, J., McKrell, T., & Hu, L. W. (2012). Measurement and model validation of nanofluid specific heat capacity with differential scanning calorimetry. *Advances in Mechanical Engineering*, 181079, 1–6

Paramatthanuwat, T., Boothaisong, S., Rittidech, S., & Booddachan, K. (2010). Heat transfer characteristics of a two-phase closed thermosyphon using de ionized water mixed with silver nano. *Heat and Mass Transfer,* 46(3), 281–285.

Parametthanuwat, T., Bhuwakietkumjohn, N., Rittidech, S., & Ding, Y. (2015). Experimental investigation on thermal properties of silver nanofluids. International Journal of *Heat and Fluid Flow*, 23(4), 317-332

Parametthanuwat, T., & Rittidech, S. (2013). Silver nanofluid containing oleic acid surfactant as working fluid in the two-phase closed thermosyphon (TPCT): A thermodynamic study. *Nanoscale and Microscale Thermophysical Engineering*, 17(3), 216-235

Parametthanuwat, T, & Rittidech, S. (2012). Heat transfer characteristics of the two-phase closed thermosyphon (TPCT) containing silver nanofluids with oleic acid surfactant, Ph.D. Thesis, Mahasarakham University, Thailand

Parametthanuwat, T., Rittidech, S., Pattiya, A., Ding, Y., & Witharana, S. (2011). Application of silver nanofluid containing oleic acid surfactant in a thermosyphon economizer. *Nanoscale Research Letters*, 6 (315), 1-10

Patel, H. E., Das, S. K., Sundararajan, T., Sreekumaran Nair, A., George, B., & Pradeep, T. (2003). Thermal conductivities of naked and monolayer protected metal nanoparticle based nanofluids: Manifestation of anomalous enhancement and chemical effects. *Applied Physics Letters*, 83(14), 2931–2933.

Payakaruk, T., Terdtoon, P., & Ritthidech, S. (2000). Correlations to predict heat transfer characteristics of an inclined closed two-phase thermosyphon at normal operating conditions. Applied Thermal Engineering, 20(9), 781–790.

Radiom, M., Yang, C., & Chan, W. K. (2013). Dynamic contact angle of water-based titanium oxide nanofluid, *Nanoscale Research Letters,* 8(282), 1–9

Ramesh, G., & Prabhu, N. K. (2011). Review of thermo-physical properties, wetting and heat transfer characteristics of nanofluids and their applicability in industrial quench heat treatment. *Nanoscale Research Letters*, 6(334), 1–15

Reay, D., & Kew, P. (2006). Heat pipe, Theory, Design And Application (Fifth edit). Butterworth-Heinemann, Oxford, United Kingdom

Ristoiu, D., Ristoiu, T., Coama, C., & Cenan, D. (2003). Experimental investigation of inclination angle on heat transfer characteristics of closed two-phase thermosyphon. 5th General Conference of the Balkan Physical, Vrnjacka Banja, Serbia, 25–29

Rittidech, S., Pipatpaiboon, N., & Terdtoon, P. (2007). Heat-transfer characteristics of a closed-loop oscillating heat-pipe with check valves. *Applied Energy,* 84(5), 565–577.

Rittidech, S., & Sangiamsuk, S. (2012). Internal Flow Patterns on Heat Transfer Performance of a Closed-Loop Oscillating Heat Pipe with Check Valves. *Experimental Heat Transfer,* 25(1), 48–57.

Sharma, P., Baek, I. H., Cho, T., Park, S., & Lee, K. B. (2011). Enhancement of thermal conductivity of ethylene glycol based silver nanofluids. Powder Technology, 208(1), 7–19.

Sözen, A., Khanları, A., & Çiftçi, E. (2019). Experimental and numerical investigation of nanofluid usage in a plate heat exchanger for performance improvement. *International Journal of Renewable Energy Development*, 8(1), 27–32

Srimuang, W., Rittidech, S., & Bubphachot, B. (2009). Heat transfer characteristics of a vertical flat thermosyphon (VFT). *Journal of Mechanical Science and Technology,* 23(9), 2548–2554.

Starace, A. K., Gomez, J. C., Wang, J., Pradhan, S., & Glatzmaier, G. C. (2011). Nanofluid heat capacities. *Journal of Applied Physics,* 10(12), 4323

Terdtoon, P., Chailungkar, M., & Shiraishi, M. (1998). Effects of Aspect Ratios on Internal Flow Patterns of an Inclined Closed Two-Phase Thermosyphon at Normal Operating Condition. *Heat Transfer Engineering*, 19(4), 75–85.

Vincent, C. C. J., & Kok, J. B. W. (1992). Investigation of the overall transient performance of the industrial two-phase closed loop thermosyphon. *International Journal of Heat and Mass Transfer,* 35(6), 1419–1426

Warrier, P., & Teja, A. (2011). Effect of particle size on the thermal conductivity of nanofluids containing metallic nanoparticles. Nanoscale Research Letters, 6(1), 1–6

Yu, W., France D.M., Choi S.U.S., & Rooutbort, J. L. (2007). Review and assessment of nanofluids technology for transportation and other application, Energy system Division,. Argonne National, Argonne, IL60439, USA., April.

Zamzamian, A., Oskouie, S. N., Doosthoseini, A., Joneidi, A., & Pazouki, M. (2011). Experimental investigation of forced convective heat transfer coefficient in nanofluids of Al2O3/EG and CuO/EG in a double pipe and plate heat exchangers under turbulent flow. *Experimental Thermal and Fluid Science*, 35(3), 495–502.